J|A|C|S ARTICLES

Published on Web 08/18/2010

Rational Design of Acridine-Based Ligands with Selectivity for Human Telomeric Quadruplexes

Silvia Sparapani, Shozeb M. Haider, Filippo Doria, Mekala Gunaratnam, and Stephen Neidle*

CR-UK Biomolecular Structure Group, The School of Pharmacy, University of London, London WC1N 1AX, U.K.

Received January 15, 2010; E-mail: stephen.neidle@pharmacy.ac.uk

Abstract: Structure-based modeling methods have been used to design a series of disubstituted triazole-linked acridine compounds with selectivity for human telomeric quadruplex DNAs. A focused library of these compounds was prepared using click chemistry and the selectivity concept was validated against two promoter quadruplexes from the *c-kit* gene with known molecular structures, as well as with duplex DNA using a FRET-based melting method. Lead compounds were found to have reduced effects on the thermal stability of the *c-kit* quadruplexes and duplex DNA structures. These effects were further explored with a series of competition experiments, which confirmed that binding to duplex DNA is very low even at high duplex:telomeric quadruplex ratios. Selectivity to the *c-kit* quadruplexes is more complex, with some evidence of their stabilization at increasing excess over human telomeric quadruplex DNA. Selectivity is a result of the dimensions of the triazole-acridine compounds, and in particular the separation of the two alkyl-amino terminal groups. Both lead compounds also have selective inhibitory effects on the proliferation of cancer cell lines compared to a normal cell line, and one has been shown to inhibit the activity of the telomerase enzyme, which is selectively expressed in tumor cells, where it plays a role in maintaining telomere integrity and cellular immortalization.

Introduction

Quadruplex nucleic acids can be formed by the folding of DNA or RNA sequences that have several repeats of short guanine-containing tracts, into structures comprising a stem of stacked G-quartets held together by loop arrangements arising from the sequences occurring between the G-tracts.[1] Quadruplex-forming sequences occur in particular at the ends of eukaryotic chromosomes, in promoter regions and/or in both 5′ and 3′ untranslated regions of a number of genes.[2] Stabilization of quadruplex structures within their genomic environments by the binding of small molecules can lead to a range of biological effects. Promoter quadruplex formation and stabilization can result in inhibition of the transcription of a targeted gene,[3] and formation of telomeric quadruplexes can inhibit the end-capping[4] and catalytic functions[5] of the telomerase enzyme from maintaining telomere integrity in cancer cells. The antitumor activity of several acridine derivatives in xenograft models, notably the molecules BRACO-19[6] and RHPS4,[7] has been ascribed to their binding to telomeric quadruplexes. However these acridines are also relatively nonselective, with significant binding affinity to duplex DNA, as well as to a

(1) Davis, J. T. *Angew. Chem., Int. Ed.* **2004**, *43*, 668. Burge, S.; Parkinson, G. N.; Hazel, P.; Todd, A. K.; Neidle, S. *Nucleic Acids Res.* **2006**, *34*, 5402. Phan, A. T.; Kuryavyi, V.; Luu, K. N.; Patel, D. J. *Nucleic Acids Res.* **2007**, *35*, 6517.

(2) Todd, A. K.; Johnston, M.; Neidle, S. *Nucleic Acids Res.* **2005**, *33*, 2901. Huppert, J. L.; Balasubramanian, S. *Nucleic Acids Res.* **2005**, *33*, 2908. Huppert, J. L.; Balasubramanian, S. *Nucleic Acids Res.* **2007**, *35*, 406. Balasubramanian, S.; Neidle, S. *Curr. Opin. Chem. Biol.* **2009**, *13*, 345.

(3) See for example: (a) Siddiqui-Jain, A.; Grand, C. L.; Bearss, D. J.; Hurley, L. H. *Proc. Natl. Acad. Sci USA* **2002**, *99*, 11593. Cogoi, S.; Xodo, L. E. *Nucleic Acids Res.* **2006**, *34*, 2536. Gunaratnam, M.; Swank, S.; Haider, S. M.; Galesa, K.; Reszka, A. P.; Beltran, M.; Cuenca, F.; Fletcher, J. A.; Neidle, S. *J. Med. Chem.* **2009**, *52*, 3774. (b) Kumari, S.; Bugaut, A.; Huppert, J. L.; Balasubramanian, S. *Nature Chem. Biol* **2007**, *3*, 218. Halder, K.; Wieland, M.; Hartig, J. S. *Nucleic Acids Res.* **2009**, *37*, 6811. Balkwill, G. D.; Derecka, K.; Garner, T. P.; Hodgman, C.; Flint, A. P.; Searle, M. S. *Biochemistry* **2009**, *48*, 11487.

(4) Gomez, D.; Wenner, T.; Brassart, B.; Douarre, C.; O'Donohue, M. F.; El, K. V.; Shin-Ya, K.; Morjani, H.; Trentesaux, C.; Riou, J. F. *J. Biol. Chem.* **2006**, *281*, 38721. Phatak, P.; Cookson, J. C.; Dai, F.; Smith, V.; Gartenhaus, R. B.; Stevens, M. F.; Burger, A. M. *Br. J. Cancer* **2007**, *96*, 1223.

(5) (a) Zahler, A. M.; Williamson, J. R.; Cech, T. R.; Prescott, D. M. *Nature* **1991**, *350*, 718. (b) Sun, D.; Thompson, B.; Cathers, B. E.; Salazar, M.; Kerwin, S. M.; Trent, J. O.; Jenkins, T. C.; Neidle, S.; Hurley, L. H. *J. Med. Chem.* **1997**, *40*, 2113. (c) Read, M.; Harrison, R. J.; Romagnoli, B.; Tanious, F. A.; Gowan, S. H.; Reszka, A. P.; Wilson, W. D.; Kelland, L. R.; Neidle, S. *Proc. Natl. Acad. Sci. U.S.A.* **2001**, *98*, 4844.

(6) Burger, A. M.; Dai, F.; Schultes, C. M.; Reszka, A. P.; Moore, M. J.; Double, J. A.; Neidle, S. *Cancer Res.* **2005**, *65*, 1489. Gunaratnam, M.; Greciano, O.; Martins, C.; Reszka, A. P.; Schultes, C. M.; Morjani, H.; Riou, J.-F.; Neidle, S. *Biochem. Pharmacol.* **2007**, *74*, 679.

(7) Salvati, E.; Leonetti, C.; Rizzo, A.; Scarsella, M.; Mottolese, M.; Galati, R.; Sperduti, I.; Stevens, M. F.; D'Incalci, M.; Blasco, M.; Chiorino, G.; Bauwens, S.; Horard, B.; Gilson, E.; Stoppacciaro, A.; Zupi, G.; Biroccio, A. *J. Clin. Invest.* **2007**, *117*, 3236.

(8) For recent surveys see: (a) Monchaud, D.; Teulade-Fichou, M. P. *Org. Biomol. Chem.* **2008**, *6*, 627. Tan, J.-H.; Gu, L.-Q.; Wu, J.-Y. *Mini-rev. Med. Chem.* **2008**, *8*, 1163. Franceschin, M. *Eur. J. Org. Chem.* **2009**, *14*, 2225. (b) Laronze-Cochard, M.; Kim, Y.-M.; Brassart, B.; Riou, J.-F.; Laronze, J.-Y.; Sapi, J. *Eur. J. Med. Chem.* **2009**, *44*, 3880. Debary, J.; Zeghida, W.; Jourdan, N.; Monchard, D.; Dheu-Andries, M.-L.; Dumy, P.; Teulade-Fichou, M.-P.; Demeunynck, M. *Org. Biomol. Chem.* **2009**, *7*, 5219. Fu, Y.-T.; Keppler, B. R.; Soares, J.; Jarstfer, M. B. *Bioorg. Med. Chem.* **2009**, *17*, 2030.

number of genomic quadruplexes. Many other quadruplex-binding small molecules have been reported,[8a] including a number of acridine-based ligands;[8b] a particular challenge is for a given ligand to have high selectivity for any chosen one over other quadruplex structures, as well as to have low affinity for duplex DNA, which is the overwhelming nucleic acid background in the genome. Structural information has revealed the presence of several distinctive topologies for telomeric quadruplexes, dependent on the nature of the cations present, and on molecular crowding conditions.[9,10] Although only a small number of ligands have been evaluated to date by structural studies, these at least generally appear to bind preferentially to parallel folded arrangements of human telomeric G-quadruplexes.[11,12]

We describe here the rational design, synthesis and evaluation of a series of novel triazole-acridine conjugates that bind with high selectivity to human telomeric quadruplex structures, as judged by interactions with intramolecular human parallel and (3 + 1) hybrid antiparallel telomeric quadruplex DNAs.[9a] Their design is based on a comparative study of the crystallographic and NMR data on these human telomeric quadruplexes and the two quadruplexes found in the promoter region of the *c-kit* gene,[13] and their selectivity is derived from differences in accessible binding site dimensions between the different quadruplexes.

Results

Molecular Modeling. Previous crystallographic analyses of quadruplex-acridine complexes[11a,14] have shown a singular binding geometry for the acridine core, stacked onto the end of the G-quartet stem of the quadruplex, with some $\pi-\pi$ overlap between two guanine bases and the acridine. This general type of arrangement was therefore taken as a starting point for subsequent modeling and structure prediction. It was initially postulated that the ring nitrogen atom of the acridine moiety would be preferentially positioned over the central ion channel in a quadruplex, and that directly attaching appropriate heterocyclic rings at the 3- and 6-positions would maximize overlap with guanine bases. Initially the ionization status of this nitrogen atom was unknown; an initial supposition that it is protonated at physiological pH was overturned by subsequent experiment (see below). We also reasoned that triazole rings would be optimal substituents at the 3- and 6-positions, because (a) they offer minimal steric resistance to coplanarity with the acridine group, and (b) their planarity and electron-richness could enhance possible $\pi-\pi$ interactions with G-quartets. A small library of end-groups[5c] was designed (each attached to a phenyl ring, to further enhance possible $\pi-\pi$ G-quartet interactions). Some variation in side-chain length has also been incorporated in order to explore a range of distances between their two distant 3- and 6-ends.

Preliminary circular dichroism studies on ligand complexes of the human telomeric quadruplex (see below) indicated that in solution they probably exist as a mixture of topologies. Thus modeling was performed on two distinct (parallel and antiparallel) topologies in order to approximate the solution situation. The coordinate files for the human telomeric quadruplex X-ray structure[9a] (PDB id 1KF1), an NMR-derived (3 + 1) hybrid antiparallel human telomeric quadruplex structure[9e] (hybrid-2, PDB id 2JPZ), together with the two *c-kit* quadruplex NMR structures (*c-kit1*, PDB id 2KQG;[13b] *c-kit2*, PDB id 203M[13c]) were used as starting-points for a series of systematic docking studies followed by short molecular dynamics simulations to find low-energy positions for each ligand bound to these quadruplexes. The (3 + 1) hybrid-2 structure was employed because it represents one of the several forms found by NMR studies in solution, and by contrast with other hybrid structures it did not require any structural modification in order to produce a ligand binding platform. It was assumed, in accord with data from crystallographic[11,14] and NMR[12,15] studies on quadruplex-ligand complexes, that the ligands bind at one or other of the terminal G-quartets in each structure. The docking thus explored both 3′ and 5′ faces of each of these three quadruplexes. In each case detailed ligand docking was focused on compounds with side-chains each containing a methylene linker with 1−3 carbon atoms, and terminating in a pyrrolidine or a diethylamine group (compounds **8a**,**b**; **9a**,**b**; **10a**,**b**). In accord with potentiometric studies, the central ring acridine nitrogen atom was not protonated during the simulations, whereas the terminal side-chain amine groups were considered to each carry a proton, and thus a positive charge.

The modeling provides estimates of relative binding energies, although these cannot reliably be compared between different quadruplexes. Modeling with the two sets of human telomeric quadruplex complexes (Table 1), indicated that compounds **9a**,**b** with two-carbon linkers overall bind consistently best to both the parallel and the (3 + 1) structure, as judged by the calculated relative binding energies. Examination of the models themselves confirms this and shows (Figure 1a,b) that the side-chains are able to make a large number of attractive close contacts with the floor and walls of the grooves in these structures, and significantly that there are few parts of the ligands that are not on contact with DNA. It does appear that the complexes with the parallel quadruplex have a slightly greater number of

(9) (a) Parkinson, G. N.; Lee, M. P. H.; Neidle, S. *Nature* **2002**, *417*, 876. (b) Phan, A. T.; Modi, Y. S.; Patel, D. J. *J. Am. Chem. Soc.* **2004**, *126*, 8710. (c) Ambrus, A.; Chen, D.; Dai, J.; Jones, R. A.; Yang, D. *Biochemistry* **2005**, *44*, 2048. (d) Ambrus, A.; Chen, D.; Dai, J.; Bialis, T.; Jones, R. A.; Yang, D. *Nucleic Acids Res.* **2006**, *34*, 2723. (e) Dai, J.; Carver, M.; Punchihewa, M.; Jones, R. A.; Yang, D. *Nucleic Acids Res.* **2007**, *35*, 4927. (f) Lim, K. W.; Amrane, S.; Bouaziz, S.; Xu, W.; Mu, Y.; Patel, D. J.; Luu, K. N.; Phan, A. T. *J. Am. Chem. Soc.* **2009**, *131*, 4301. (g) Haider, S. M.; Parkinson, G. N.; Neidle, S. *Biophys. J.* **2008**, *95*, 296. Haider, S. M.; Neidle, S. *Biochem. Soc. Trans.* **2009**, *7*, 583.

(10) Xue, Y.; Kan, Z. Y.; Wang, Q.; Yao, Y.; Liu, J.; Hao, Y. H.; Tan, Z. *J. Am. Chem. Soc.* **2007**, *129*, 11185. Renciuk, D.; Kejnovská, I.; Skoláková, P.; Bednárová, K.; Motlová, J.; Vorlícková, M. *Nucleic Acids Res.* **2009**, *37*, 6625. Zheng, K.-W.; Chen, Z.; Hao, Y.-H.; Tan, Z. *Nucleic Acids Res.* **2010**, *38*, 327. Martino, L.; Pagano, B.; Fotticchia, I.; Neidle, S.; Giancola, C. *J. Phys. Chem. B* **2009**, *113*, 14779.

(11) (a) Parkinson, G. N.; Ghosh, R.; Neidle, S. *Biochemistry* **2007**, *46*, 2390. (b) Parkinson, G. N.; Cuenca, F.; Neidle, S. *J. Mol. Biol.* **2008**, *381*, 1145. (c) Campbell, N. H.; Parkinson, G. N.; Reszka, A. P.; Neidle, S. *J. Am. Chem. Soc.* **2008**, *130*, 6722.

(12) Phan, A. T.; Kuryavyi, V.; Gaw, H. Y.; Patel, D. J. *Nature Chem. Biol.* **2005**, *1*, 167.

(13) (a) Rankin, S.; Reszka, A. P.; Huppert, J.; Zloh, M.; Parkinson, G. N.; Todd, A. K.; Ladame, S.; Balasubramanian, S.; Neidle, S. *J. Am. Chem. Soc.* **2005**, *127*, 10584. Phan, A. T.; Kuryavyi, V.; Burge, S.; Neidle, S.; Patel, D. J. *J. Am. Chem. Soc.* **2007**, *129*, 4386. (b) Fernando, H.; Reszka, A. P.; Huppert, J.; Ladame, S.; Rankin, S.; Venkitaraman, A. R.; Neidle, S.; Balasubramanian, S. *Biochemistry* **2006**, *45*, 7854. (bb) Phan, A. T.; Kuryavyi, V.; Burge, S.; Neidle, S.; Patel, D. J. *J. Am. Chem. Soc.* **2007**, *129*, 4386. (c) Hsu, S. T.; Varnai, P.; Bugaut, A.; Reszka, A. P.; Neidle, S.; Balasubramanian, S. *J. Am. Chem. Soc.* **2009**, *131*, 13399.

(14) Haider, S. M.; Parkinson, G. N.; Neidle, S. *J. Mol. Biol.* **2003**, *326*, 117. Campbell, N. H.; Patel, M.; Tofa, A. B.; Ghosh, R.; Parkinson, G. N.; Neidle, S. *Biochemistry* **2009**, *48*, 1675.

(15) Gavathiotis, E.; Heald, R. A.; Stevens, M. F.; Searle, M. S. *J. Mol. Biol.* **2003**, *334*, 25.

Table 1. Calculated Binding Energies for Selected Compounds to the Two Telomeric Quadruplex Structures, to the Two *c-kit* Promoter Quadruplexes, and to a 45-mer

	$\Delta E_{binding}$ (kcal mol^{-1})				
compound	parallel G4	(3 + 1) G4	*c-kit1*	*c-kit2*	45-mer G4
8a	−14.0	−19.3	−8.0	−7.0	−24.3
8b	−19.2	−22.7	−8.2	−7.0	−26.0
9a	−19.5	−25.2	−8.4	−6.8	−29.1
9b	−19.4	−23.8	−8.3	−7.1	−27.5
10a	−12.3	−17.8	−8.1	−7.0	−23.4
10b	−12.2	−16.3	−8.0	−7.1	−23.1

contacts, suggesting that this may be the preferred form, but experimental verification will have to await a crystal structure. The more compact shape of the hybrid structure means that part of one ligand side-chain is unable to fully contact the quadruplex surface (Figure 1b). We have also examined the binding of the molecules to a 45-mer model of human telomeric DNA, with two consecutive quadruplexes and a single ligand binding site between them.[9g] This arrangement may be a more realistic model for ligand binding to the human telomere than a single quadruplex. The ranking order of ligand binding (Table 1) for the 45-mer is the same as those for the other telomeric quadruplexes.

The modeling also clearly indicates that compound **9a** cannot bind as effectively to the *c-kit1* quadruplex (Figure 1c). There are extensive steric clashes when it is bound at the 5′ end of the quadruplex, which push the central acridine chromophore away from the G-quartets while the side-chains of the ligand cannot interact fully with the backbone atoms. At the 3′ end the optimal position of the ligand is such that its termini are unable to make effective contacts with the single-residue loop of the quadruplex. An analogous situation occurs with the *c-kit2* quadruplex (Figure 1c). In this instance the ends of the side-chains are too long to be able to fit into the loop structure and protrude outward. Ligands with one- or three-carbon linkers, series **8a**−**i** and **10a**−**i** (see Scheme 1) have also been modeled, and similarly, these are also predicted to not bind as effectively to these two quadruplexes. No low-energy arrangement was found for duplex DNA binding to compound **9a** (or indeed any others in the series), using either an intercalation site or groove binding model.

Synthesis of Ligands. The 3,6-diazoacridine **2** was readily obtained by diazotization of the readily available 3,6-aminoacridine **1**, as previously reported.[16] The straightforward synthesis of intermediates **5a**−**i** and **6a**−**i** was accomplished in one step by reaction of the commercially available 3-ethynylaniline **3** with the appropriate acid chloride and different cyclic and aliphatic amines (see Scheme 1). The same approach was also possible with longer side chains ($n = 3$), as in the case of compounds **7a**−**i**. However, from initial attempts it was observed that yields were affected by the formation of elimination products. Their isolation from the reaction mixture, followed by subsequent amination, was necessary to force formation of the final intermediates **7a-i.** In order to circumvent the problem, the presence of unreacted materials was reduced by a two-step reaction, which involved acylation of **3** with 4-chlorobutyryl chloride in the presence of $NaHCO_3$ at 0 °C, prior to aminolysis of **4** with the required amine under mild thermal conditions, to afford compounds **7a**−**i** in good yields. The target ligands **8a**−**i**, **9a**−**i**, and **10a**−**i** were synthesized by Cu(I) catalyzed Huisgen 1,3-dipolar cycloaddition between bisazide **2** and alkyne building blocks **5a**−**i** through **7a**−**i**. The "click" reaction[17] was performed under typical conditions, using $CuSO_4 \cdot 5H_2O$ and sodium ascorbate in a 1:1 mixture of t-BuOH/H_2O, with stirring for 72 h and at room temperature. Attempts to increase the rate of reaction by thermolysis or microwave irradiation were unsuccessful, due to the formation of unidentified degradation products, as revealed by LC/MS analysis. The reactions proceeded smoothly and final bis-triazole derivatives that precipitated in water were initially isolated by filtration and ultimately purified by semipreparative HPLC.

Ligand Protonation Status. The 9-position of many 3,6-disubstituted acridines such as the diamino compound 1, is normally protonated at physiological pH. In order to assess the effect of the direct attachment of the triazole rings to the 3- and 6-positions, a potentiometric method was used to obtain pK_a values. The titration of NaOH with (arbitrarily chosen) compound **10a** shows two points of inflection (Figure 2a), which analysis show (Figures 2b,c) correspond to pK_a values of 4.03 ± 0.03 and 8.54 ± 0.10, respectively. We interpret this in terms of two distinct protonation categories, the two equivalent terminal amines having a pK_a value of 8.54, whereas the lower value of 4.03 corresponds to the acridine ring nitrogen atom, which is therefore not protonated under physiologically relevant conditions.

Solution Binding Studies. The CD spectra of the human 22-mer telomeric quadruplex (Figure 3a,b) in the presence of increasing concentrations of one of the ligands (**9b**) in K^+ and Na^+ solution, show characteristics typical of quadruplex behavior, although the two spectra show distinct maxima. The spectra in Na^+ solution show a prominent peak at 295 nm, consistent with an antiparallel structure, which is retained on titrating increasing equivalents of ligand. The spectra in K^+ solution show a strong shoulder at ca. 260−265 nm and a major peak at 290 nm, consistent with a mixed population of parallel and (probably several) antiparallel species, as has been observed in a number of previous studies with ligands binding to human telomeric quadruplexes.[18,19] It is apparent that, at least under the solution conditions of a typical CD experiment, that different ligands can stabilize or induce differing topologies, with some inducing a parallel fold, such as the oxazine compound oxazine170,[20] several amido phthalocyanines[21] and diarylethynyl amides.[22]

Compounds were assessed for their ability to stabilize the melting temperature (T_m) of all three quadruplexes and a DNA duplex, using a fluorescence resonance energy transfer (FRET) procedure[23] (Table 2). This shows that the two-methylene linker

(16) Kanakarajan, K.; Haider, K.; Czarnik, A. W. *Synthesis* **1988**, *7*, 566.
(17) Rostovtsev, V. V.; Green, L. G.; Fokin, V. V.; Sharpless, K. B. *Angew. Chem., Int. Ed.* **2002**, *41*, 2596.
(18) See for example: Shirude, P. S.; Gillies, E. R.; Ladame, S.; Godde, F.; Shin-ya, K.; Huc.;Balasubramanian, S. *J. Am. Chem. Soc.* **2007**, *129*, 11890. Li, G.; Huang, J.; Zhang, M.; Zhou, Y.; Zhang, D.; Wu, Z.; Wang, S.; Weng, X.; Zhou, X.; Yang, G. *Chem. Commun.* **2008**, 4564. Tera, M.; Ishizuka, H.; Takagi, M.; Suganuma, M.; Shin-ya, K.; Nagasawa, K. *Angew. Chem., Int. Ed.* **2008**, *47*, 1.
(19) Garner, T. P.; Williams, H. E. L.; Gluszyk, K. I.; Roe, S.; Oldham, N. J.; Stevens, M. F. G.; Moses, J. E.; Searle, M. S. *Org. Biomol. Chem.* **2009**, *7*, 4194.
(20) Chen, M.; Song, G.; Wang, C.; Hu, D.; Ren, J.; Qu, J. *Biophys. J.* **2009**, *97*, 2014.
(21) Alzeer, J.; Luedtke, N. W. *Biochemistry* **2010**, *49*, 4339.
(22) Dash, J.; Shirude, P. S.; Hsu, S. D.; Balasubramanian, S. *J. Am. Chem. Soc.* **2008**, *130*, 16048.
(23) Schultes, C. M.; Guyen, B.; Cuesta, J.; Neidle, S. *Bioorg. Med. Chem. Lett.* **2004**, *14*, 4347. Guédin, A.; Lacroix, L.; Mergny, J.-L. *Methods Mol. Biol.* **2010**, *613*, 25.

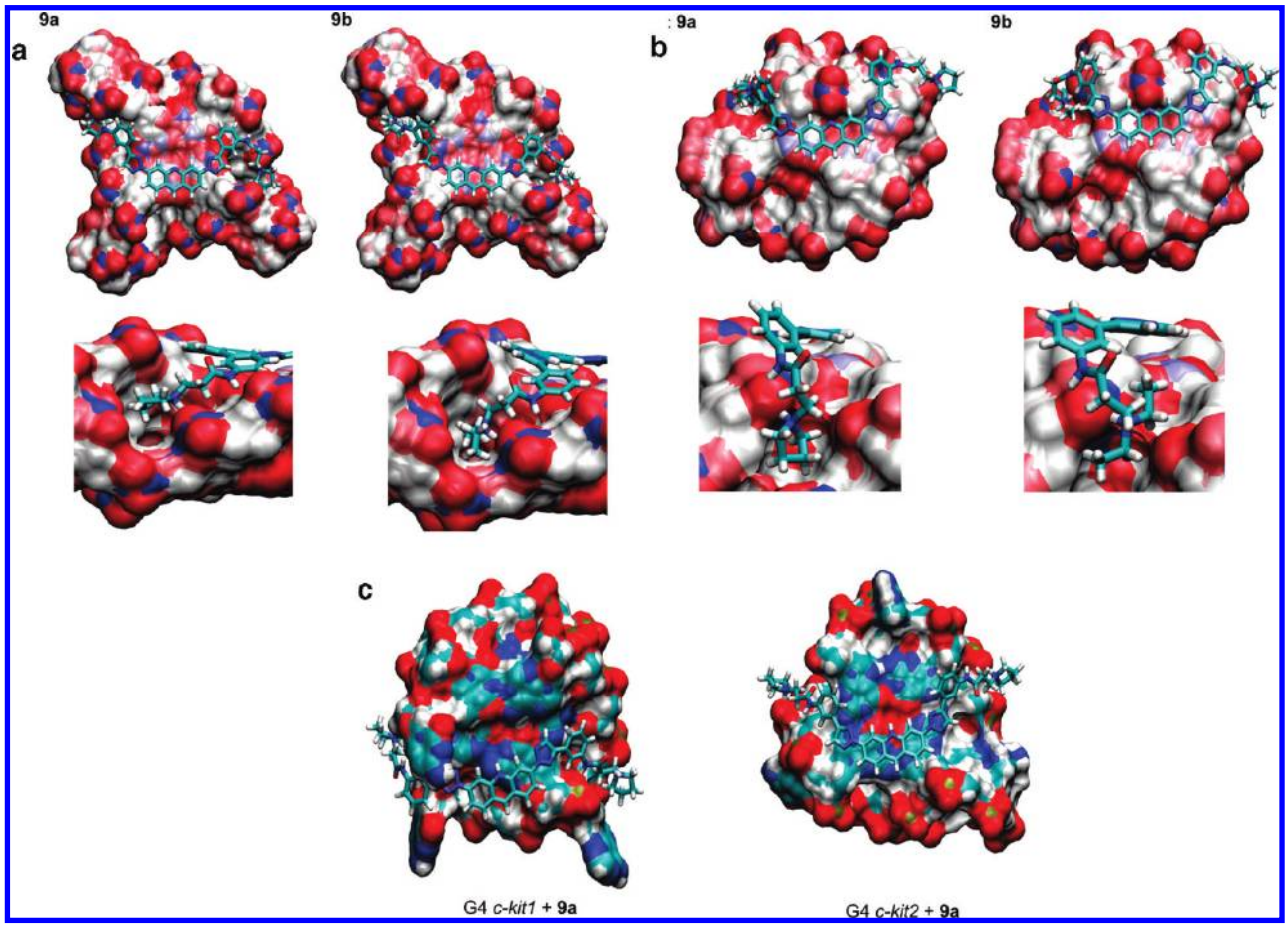

Figure 1. (a) Views of the docked low-energy positions of ligands **9a** and **9b** on the parallel-stranded human telomeric quadruplex. The upper views show the position of each ligand in stick representation stacking onto the terminal G-quartet, shown as a solvent-accessible surface. The lower views show the positively charged side-chains of each ligand accessing the propeller loops and interacting with the negatively charged sugar phosphate backbone. (b) Views of the docked low-energy positions of ligands **9a** and **9b** on the antiparallel (3 + 1) hybrid human telomeric quadruplex. The lower views show side-chains of the ligands accessing the grooves formed by the distinctive (3 + 1) antiparallel topology. (c) Views of the docked low-energy positions of ligand **9a** bound to the *c-kit1* and *c-kit2* quadruplexes. In the *c-kit1* complex, the shape of the ligand ring system positions the side-chains in close vicinity to the backbone, resulting in steric repulsion. In the *c-kit2* complex there are two single-nucleotide loops and one five-nucleotide loop. The conformations adopted by these loops prevent the side-chains from making favorable interactions with them.

Scheme 1. Synthesis of Triazole-Linked Acridines

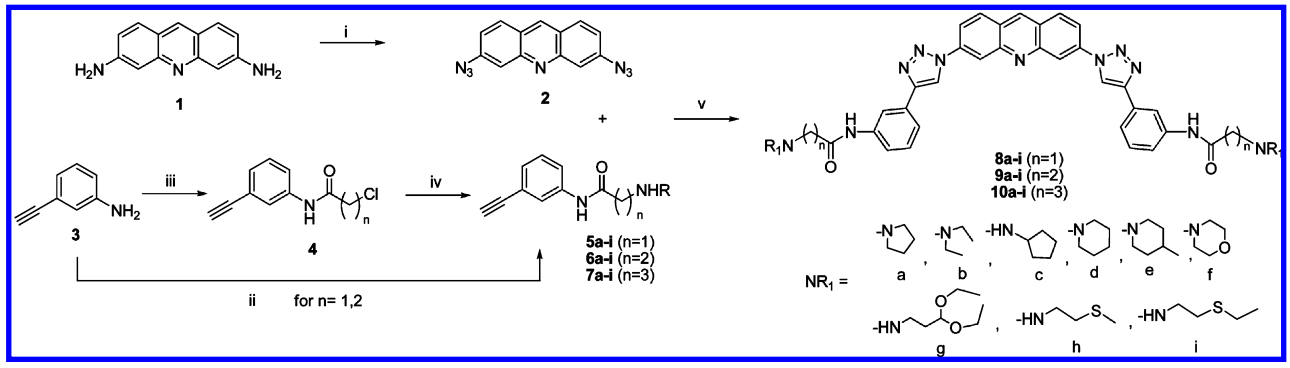

series that two compounds, **9a** and **9b**, have ΔT_m values >12 °C, and one other, **9d**, has a ΔT_m > 6 °C with the human telomeric quadruplex. This suggests that the size of the cationic group at the terminus of the side chains has a significant effect on binding, and the pyrrolidine ring in **9a** (and the equivalent in **9b**), is an optimal size, in accord with the findings of the modeling that the groove pocket in both telomeric quadruplexes modeled here is relatively small and would require distortion to accommodate larger groups.

Only one compound in the series, the morpholino derivative **9f**, has a significant effect on duplex DNA stability; by contrast all the other compounds have ΔT_m values with duplex that are essentially 0 °C within the limits of the sensitivity of the FRET method. G4 selectivity vs duplex DNA has been further assessed by a series of FRET-based competition assay for the two approximately equipotent ligands **9a** and **9b**, which shows that increasing duplex:quadruplex ratios, result in almost complete retention of their G4 stabilizing ability (Figure 4a), with <10%

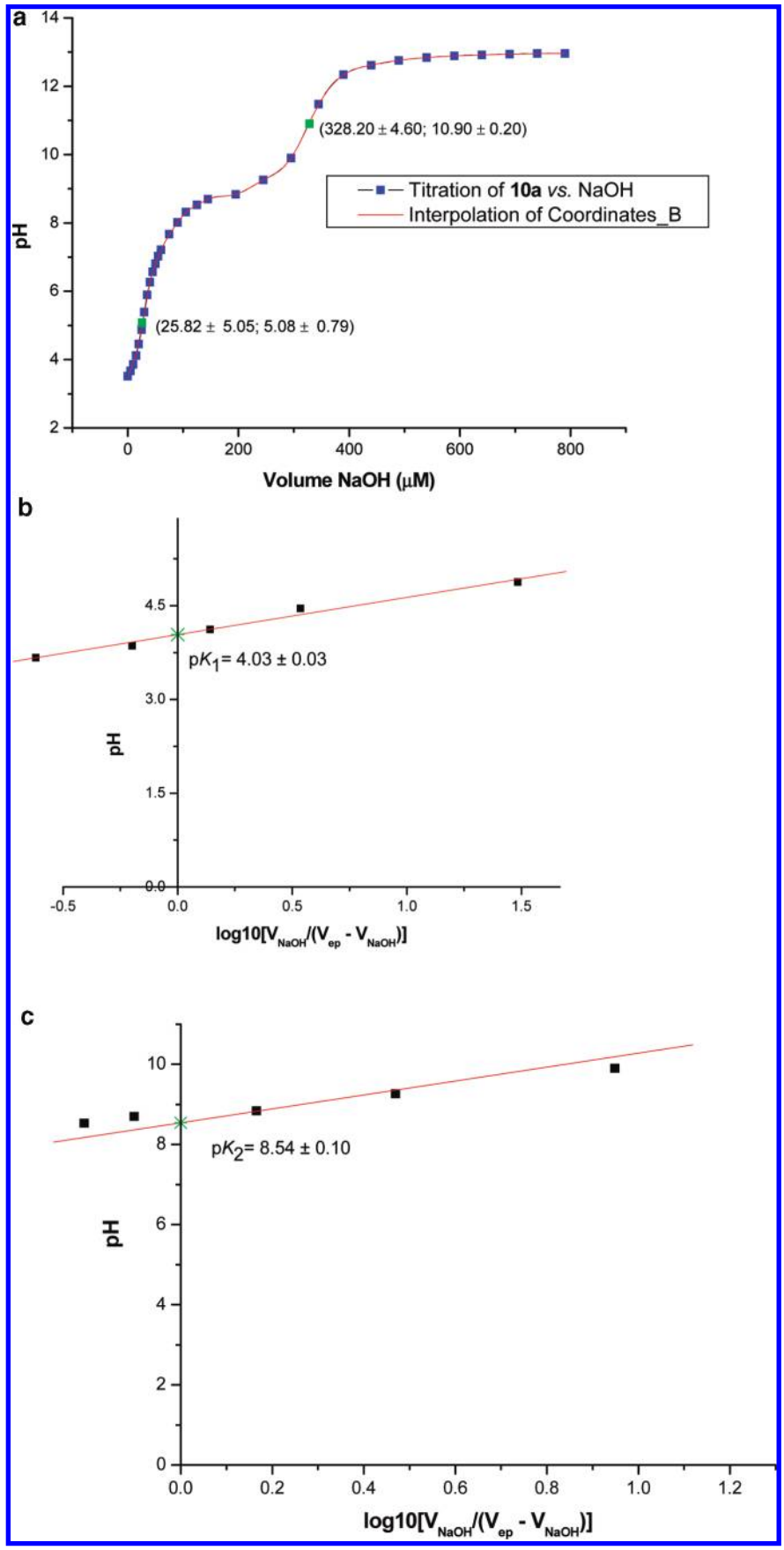

Figure 2. Titration curves for compound **10a** with 0.1 M NaOH, (a) showing the two inflection points produced with increasing volume with respect to pH, and (b,c) showing the straight lines produced by multiple linear regression analysis of the pH vs equilibrium constant plot to give the two pK_a values.

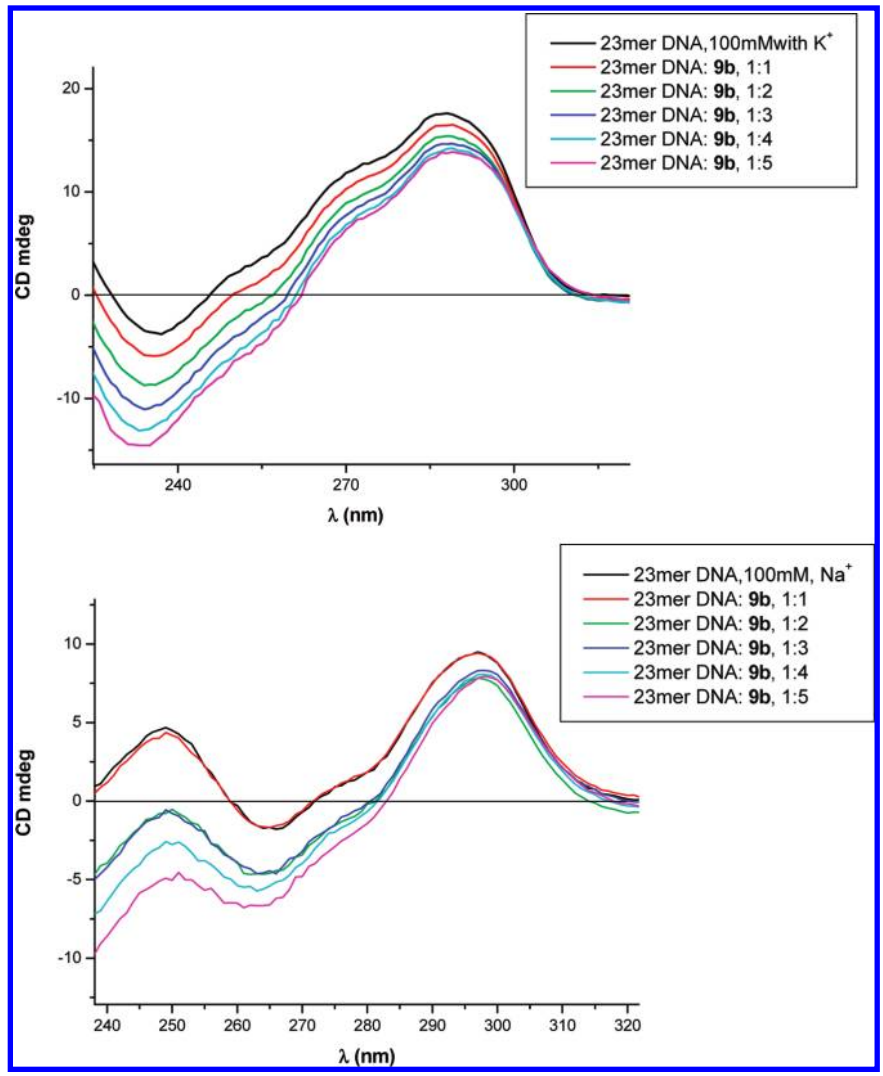

Figure 3. Circular dichroism spectra for compound **9b** titrated against the 23-mer human intramolecular telomeric quadruplex (top) in 100 mM Na^+ solution and (bottom) in 100 mM K^+ solution.

change in ΔT_m values at the highest, 300-fold excess of duplex DNA that was employed.

Interactions with the *c-kit1* and *c-kit2* quadruplexes are generally weak, and for compounds **9a** and **9b**, are on the borderline of significance, as assessed by their ΔT_m values. Competition assays with the human telomeric quadruplex vs the *c-kit1* and *c-kit2* quadruplexes show a more complex picture (Figure 4b−d). The results with increasing ratios of the *c-kit2* quadruplex are surprising (Figure 4c) since they show ΔT_m values increasing beyond a ratio of 1:10. ΔT_m values in the absence of ligand, of 5.4 °C at a 1:100 excess and 9.2 °C at a 1:300 excess of *c-kit2* sequence indicate that the *c-kit2* quadruplex sequence itself is stabilizing the human telomeric sequence, possibly by forming an intermolecular quadruplex. Accordingly the competition data was normalized by subtracting the ΔT_m values solely due to stabilization of the human telomeric quadruplex-*c-kit2* interaction, to give Figure 4d, which shows that these ligands are interacting, now with the *c-kit2* quadruplex, as with *c-kit1*. These results suggest that, contrary to the suggestion from the low ΔT_m values with the *c-kit1* and *c-kit2* quadruplex alone, these ligands do not have negligible affinity for them.

Alterations of the side chains to one or three CH_2− groups (series **8a**−**i** and **10a**−**i**) as well as changes in their basicity, do not result in any positive stabilizing effects. The trisubstituted acridine compound BRACO-19, which in common with **9a**, has basic pyrrolidino group at positions 3 and 6, does bind to the human telomeric quadruplex with high affinity. However this is at the cost of selectivity. Thus BRACO-19 stabilizes all three quadruplexes to an approximately equal extent, and has significant interaction with duplex DNA.

Telomerase Activity and Inhibition of Cell Growth. The finding that compounds **9a**, **9b** can bind selectively to human telomeric quadruplexes suggests that they may have biological activity as telomerase inhibitors. Their effects on cell proliferation have been examined using a standard SRB assay. Three human carcinoma cell lines (A549, lung; A2780, ovarian; Panc1, pancreatic) were used, together with a normal cell fibroblast line (WI38). Table 3 shows that both compounds have activity in the low μM range with at least one of the carcinoma lines; neither shows significant activity against the normal cell line. All three carcinoma lines express the telomerase enzyme at elevated levels, and the inhibitory ability of one compound, **9a**, was examined using a modified TRAP assay,[18] which showed a significant level of inhibition, and a $^{tel}IC_{50}$ of ca. 35 μM.

Discussion

The structure-based design process described here has resulted in a series of compounds with high selectivity for telomeric

Table 2. ΔT_m Data (°C) for the Acridine Ligand BRACO-19 and Compounds Reported Here, at a 1 μM Concentration and in 100 mM KCl Salt, with the Human Telomeric Quadruplex (htel), the Two *c-kit* Promoter Quadruplexes, and a Duplex (ds) DNA Sequence, Using the FRET Method[a]

	htel G4	*c-kit1* G4	*c-kit2* G4	ds DNA
BRACO-19	25.9 ± 0.2	20.1 ± 0.3	25.3 ± 0.4	11.2 ± 0.6
8a	4.0 ± 0.5	1.8 ± 0.5	4.3 ± 0.1	0.3 ± 0.1
8b	6.2 ± 0.6	1.5 ± 0.2	3.2 ± 0.8	0.2 ± 0.8
8c	1.5 ± 0.1	1.6 ± 0.2	3.5 ± 0.4	0.1 ± 0.6
8d	3.8 ± 0.8	1.0 ± 0.8	3.0 ± 0.5	0.5 ± 0.3
8e	3.5 ± 0.3	2.0 ± 0.7	3.2 ± 0.5	0.4 ± 0.0
8f	2.5 ± 0.0	0.1 ± 0.1	3.1 ± 0.4	0.4 ± 0.5
9a	15.8 ± 0.7	0.8 ± 0.2	1.4 ± 0.5	0.4 ± 0.2
9b	15.5 ± 0.6	0.7 ± 0.5	2.5 ± 0.0	0.6 ± 0.0
9c	2.8 ± 0.2	2.1 ± 0.6	2.2 ± 0.1	0.0 ± 0.1
9d	6.7 ± 0.4	2.4 ± 0.2	4.6 ± 0.3	0.1 ± 0.2
9e	4.5 ± 0.3	1.3 ± 0.1	3.4 ± 0.1	0.2 ± 0.5
9f	2.6 ± 0.6	0.0 ± 0.6	6.5 ± 1.0	5.5 ± 0.6
9g	3.0 ± 0.5	0.5 ± 0.6	6.3 ± 0.3	0.4 ± 0.5
9h	1.7 ± 0.2	0.7 ± 0.5	2.4 ± 0.9	0.0 ± 0.3
9i	0.4 ± 0.2	0.4 ± 0.3	0.4 ± 0.7	0.1 ± 0.5
10a	3.5 ± 0.5	0.4 ± 0.5	0.2 ± 0.2	0.1 ± 0.3
10c	0.9	0.6	3.8	0.3
10d	3.1	0.6	0.2	0.1
10e	1.7	0.2	0.9	0.7
10f	0.7	0.8	0.6	1.2
10h	2.3	0.2	2.2	0.1
10i	2.1	2.0	2.3	0.3

[a] A small number of ligands were not able to be purified to a sufficient extent to be analyzed by FRET and are not reported here.

quadruplex DNA over duplex DNA, and of a lead compound, **9a**, with significant telomerase inhibitory activity (although we have as yet to definitively demonstrate that this inhibition is due to induction of a quadruplex structure in the telomeric DNA primer). It is notable that compounds **9a**, **9b** are active inhibitors of cellular proliferation in at least one cancer cell line yet do not show comparable activity (>10-fold less) against a normal fibroblast cell line, which does not express telomerase. The observed selectivity of these compounds for the parallel and a (3 + 1) hybrid human telomeric quadruplex over the two parallel topology *c-kit* quadruplexes is in accord with the modeling analysis and is due to differences in loop sequence and geometry, at least on the basis of the modeling presented here. The competition studies do also suggest that single-point ΔT_m values are not by themselves reliable indicators of selectivity. For compounds **9a**, **9b** selectivity is limited to low telomeric quadruplex:*c-kit* quadruplex ratios. In potential therapeutic terms this may not be a problem since per cell there maybe just one *c-kit1* and one *c-kit2* quadruplex on the basis that the *c-kit* gene occurs uniquely in the human genome. By contrast, each human cell contains 46 × 2 single-stranded 3′ telomeric DNA ends, so telomeric quadruplexes would be at least in 100-fold excess.

An increasing number of other promoter quadruplexes have been reported,[2,3] although detailed structural data is as yet only available for a very few. Most have parallel folds, with diversity in the loops and thus asymmetry in the 3′ and 5′ ends. The same principles of ligand selectivity would apply as determined here. It is thus realistic to use a given quadruplex geometry as the basis for the design of particular analogues of the triazole-acridines or other ligands such as diarylethynyl amides[22] or nonpolycyclic triazoles[25] with selectivity for a given promoter quadruplex, and to design out telomeric quadruplex affinity by judicious changes in the side-chains.

Experimental Section

DNA Melting Experiments Using Fluorescence Resonance Energy Transfer (FRET). Dual labeled oligonucleotides (Eurogentec Ltd., U.K.) with the following sequences were used (where FAM is the donor fluorophore 6-carboxyfluorescein and TAMRA is the acceptor 6-carboxytetramethylrhodamine):

G4 DNA, 5′-*FAM*-GGGTTAGGGTTAGGGTTAGGGTTAGGG-*TAMRA*-3′

dsDNA, 5′-*FAM*-TATAGCTATATTTTTTTATAGCTATA-*TAMRA*-3′

c-kit1, 5′-*FAM*-AGAGGGAGGGCGCTGGGAGGAGGGGCT-*TAMRA*-3′

c-kit2, 5′-*FAM*-CCCGGGCGGGCGCGAGGGAGGGGAGG-*TAMRA*-3′

Each oligonucleotide was initially diluted to 100 μM in nuclease-free water (not DEPC-treated), purchased from Ambion Applied Biosystems, UK. Stock solution of 20 μM and subsequent dilutions were obtained in FRET buffer (60 mM KCl, K cacodylate, pH 7.4). Oligonucleotides at concentrations of 400 μM were annealed by heating at 85 °C for 10 min and cooled to room temperature. Original compounds were prepared as 10 mM DMSO stock solutions and diluted to 1 mM using 1 mM HCl in HPLC grade water. The rest of the dilutions were performed using FRET buffer. Next, 50 μL of annealed DNA and 50 μL of compound solution were distributed across 96-well RT-PCR plates (Bio-Rad) (MJ Research, Waltham, MA) and processed in a DNA Opticon Engine (MJ Research). All experimental values were determined in triplicate. Fluorescence readings were taken at intervals of 0.5 °C over the range 30−100 °C, with a constant temperature being maintained for 30 s prior to each reading. The incident radiation was 450−495 nm and the detection was conducted at 515−545 nm. The raw data were imported into the Origin program (version 7.0, Origin Lab Corp.) and the graphs were smoothed using a 10-point running average and subsequently normalized. All data were analyzed with the Origin Pro 7.0 software package (Origin Lab Corp., Northampton, MA). The change in melting temperature at a 1 μM ligand concentration ($\Delta T_m(1\mu M)$) was calculated from three experiments by subtraction of the blank from the averaged 1 μM ligand melting temperature.

FRET Competition assays were performed in a similar manner. Compound dilutions were prepared in concentrations four times the final ones and added as 25 μL aliquots. To G4 DNA (50 μL), ligand (25 μL, 4 μM), and the appropriate competitor calf thymus DNA (Sigma-Aldrich, UK) or unlabeled c-*kit1* or c-*kit2* oligonucleotides (25 μL), synthesized in-house, were added at the following concentration ratios of 1:1, 1:10, 1:100, 1:300 (G-quartets: pair of bases when calf thymus DNA was used). The percentage of retained F21T melting temperatures (ΔT_m) upon addition of increasing concentrations of competitor was averaged from three experiments, normalized with standard deviation to the $\Delta T_m(1\ \mu M)$ for that ligand in the absence of competitor.

Circular Dichroism (CD) Studies. CD spectra of the 23mer DNA in sodium and potassium phosphate buffers were measured on the Applied Photophysics Ltd. (Leatherhead, UK) Chirascan/Plus spectrometers at King's College, London. The CD spectra were measured between 340 and 200 nm at room temperature in a strain-free rectangular 5 mm cell. The instrument was flushed continuously with pure evaporated nitrogen throughout the measurements. Spectra were recorded with a 1 nm step size, a 1.5 s measurement time-per-point and a spectral bandwidth of 1 nm. CD experiments were carried out on annealed 23-mer human telomeric DNA sequence at a concentration of 4.4 μM DNA. Annealing was performed by heating to 85 °C for 10 min in the appropriate 100 mM sodium or potassium phosphate buffer solution, pH 7.4, followed by cooling overnight. Concentration of the ligand **9b** was determined using the recorded value of the absorbance at 260 nm by using the

(24) Reed, J. E.; Gunaratnam, M.; Beltran, M.; Reszka, A. P.; Vilar, R.; Neidle, S. *Anal. Biochem.* **2008**, *380*, 99.
(25) Moorhouse, A. D.; Santos, A. M.; Gunaratnam, M.; Moore, M.; Neidle, S.; Moses, J. E. *J. Am. Chem. Soc.* **2006**, *128*, 15972.

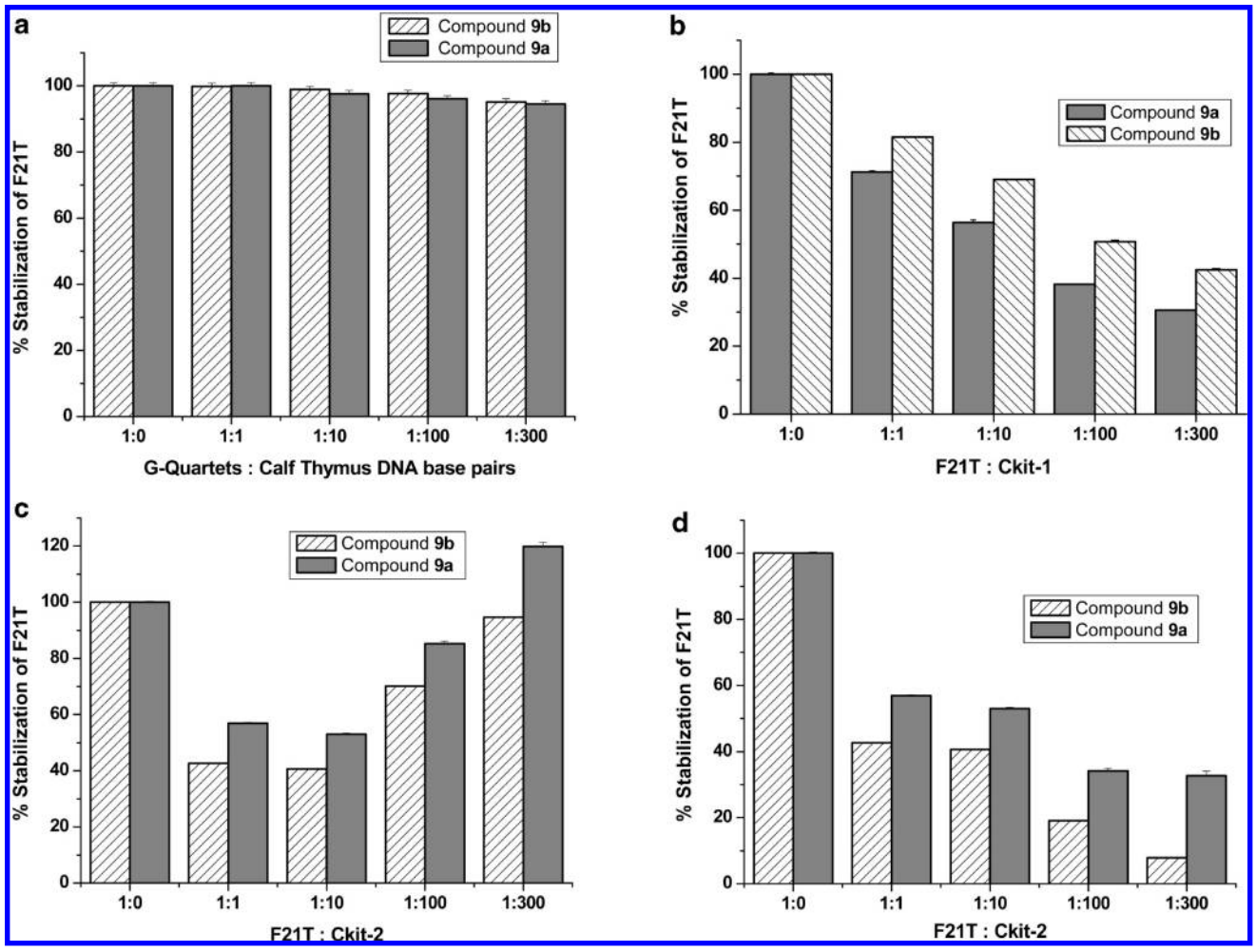

Figure 4. Competition experiments showing the effects of compounds **9a**, **9b** on the thermal stabilization of the human telomeric quadruplex, as measured by the FRET method, (a) using increasing ratios of duplex DNA (as base pairs), (b) with increasing ratios of *c-kit1* oligonucleotide (as base pairs), (c) with increasing ratios of *c-kit2* oligonucleotide (as base pairs), (d) as in (c) but now normalized by subtracting the ΔT_m values solely due to stabilization of the human telomeric quadruplex-*c-kit2* interaction.

Table 3. Quantitation of the Inhibition of Cell Proliferation by Two Selected Compounds, in Three Human Cancer Cell Lines (A549, A2780 and Panc1) and a Normal Fibroblast Line (WI38), shown as IC_{50} values (μM)

compound	A549	A2780	Panc1	WI38
BRACO-19	2.4 ± 1.0	2.5 ± 0.9	ND	10.7 ± 0.6
9a	31.4 ± 0.5	6.6 ± 0.6	$>50 \pm 2$	$>50 \pm 2$
9b	$>50 \pm 2$	4.4 ± 0.8	5.3 ± 1.0	$>50 \pm 2$

Beer−Lambert law. All raw data were and analyzed with OriginPro 7.0 software package (Origin Lab Corp., Northampton, MA) and spectra were buffer baseline corrected.

Potentiometric Titrations. A 10 mM stock solution in DMSO of compound **10a** was diluted to 5 mM with deionized water and titrated with a 0.1 M NaOH solution, previously standardized with potassium hydrogen phthalate ($V_{ep} = 0.66$ mL), starting with 5 μL additions until the first end-point region and then with increments of 15−50 μL near the second end-point region. Titrations were carried out using a glass-body pH semi-micro electrode (Hanna Instruments Ltd.). Data points were interpolated and curves were smoothed using the Boltzmann equation to determine end-point values. Dissociation constants were obtained by multiple linear regression analysis. Data were analyzed with the OriginPro 7.0 software package (Origin Lab Corp., Northampton, MA).

Molecular Modeling. The crystal structures of the 22-mer parallel-stranded propeller-loop topology (PDB 1KF1; resolution 2.10 Å) human telomeric G-quadruplex, the NMR structure of the (3 + 1) human telomeric G-quadruplex and NMR structures of the intramolecular G-quadruplexes from the promoter sequence of the human *c-kit* gene (*c-kit1* (PDB 2O3M) and *c-kit2* (PDB 2KQG)) were obtained from the Protein Data Bank and used as a starting point to examine plausible interactions with the ligands. The molecular models for the triazole-acridine series of ligands were constructed, minimized and partial charges calculated semiempirically using the MOPAC program[26] from the Insight suite software (www.accelrys.com). Prior to docking on the human telomeric quadruplex crystal structure, the extreme 5′ terminal residue was removed in order to expose the flat planar quartet to the ligand. The ligands were minimized and docked on both 5′ and 3′ surfaces of the four G-quadruplex structures using the AFFINITY docking program (www.accelrys.com), employing the grid docking method available with AFFINITY. This approach has been validated in previous studies on the rational design of quadruplex ligands.[27] The automated docking process identifies and ranks positions based on high interaction energies within the binding site. The complexes were then subjected to 1000 steps of molecular mechanics minimization and 200 ps of molecular dynamics simulations in explicit solvent at 300 K using the DISCOVER3 program in the Insight II suite software. The data was visualized by means of the

(26) Stewart, J. J. P. *J. Comput. Aided Mol. Des.* **1990**, *4*, 100.
(27) Moore, M. J.; Schultes, C. M.; Cuesta, J.; Cuenca, F.; Gunaratnam, M.; Tanious, F. A.; Wilson, W. D.; Neidle, S. *J. Med. Chem.* **2006**, *49*, 582.

VMD program.[28] Electrostatic contributions to the overall binding energy were calculated using the APBS software, employing an implicit solvent model.[29] The docked complexes were prepared using the PDB2PQR server (http://agave.wustl.edu/pdb2pqr). Charges, atom types and radii were assigned to each ligand atom based on the AMBER force field. The complexes were then subjected to APBS electrostatic calculations. A dielectric constant of 2, a solvent dielectric constant of 80 were used, together with grid spacing that were all optimally chosen such that the grid was always finer than 0.5 Å. The remaining parameters were kept at default values. The binding free energies were calculated on the basis of the simple thermodynamics cycle.

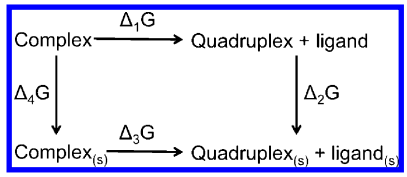

where [complex, quadruplex, ligand] and [complex$_{(s)}$, quadruplex$_{(s)}$, ligand$_{(s)}$] represent the nonsolvated and solvated states of the system respectively. The program APBS calculates binding free energies using the equation:

$$\Delta G_{\text{binding}} = -\Delta_3 G = \Delta_4 G - d\Delta_1 G - \Delta_2 G$$

This binding free energy cycle illustrates binding in terms of the transfer of free energies from a homogeneous dielectric environment to an inhomogenous dielectric environment with differing internal and external dielectric constants.[29]

Telomerase Inhibition Assay. The telomerase repeat amplification protocol (TRAP) assay was modified from a two-step to the three-step TRAP-LIG procedure:[24] step 1, initial primer elongation by telomerase and addition of ligand; step 2, subsequent removal of the ligand; step 3, PCR amplification of the products of telomerase elongation. *Step 1*: This was carried out by preparing a master mix containing the TS forward primer (0.1 μg; 5′-AAT CCG TCG AGC AGA GTT-3′), TRAP buffer (20 mM Tris-HCl [pH 8.3], 68 mM KCl, 1.5 mM $MgCl_2$, 1 mM EGTA, 0.05% v/v Tween-20), bovine serum albumin (0.05 μg), and dNTPs (125 μM each), protein extract (500 ng/sample) diluted in lysis buffer (10 mM Tris-HCl, pH 7.5, 1 mM $MgCl_2$, 1 mM EGTA, 0.5% CHAPS, 10% glycerol, 5 mM β-mercaptoethanol, 0.1 mM AEBSF). The PCR master mix was added to tubes containing freshly prepared ligand at various concentrations and to a negative control containing no ligand. The initial elongation step was carried out for 10 min at 30 °C, followed by 94 °C for 5 min and a final maintenance of the mixture at 20 °C. *Step 2*: To purify the elongated product and to remove the bound ligands the QIA quick nucleotide purification kit (Qiagen) was used according to the manufacturer's instructions. This kit is especially designed for the purification of both double and single-stranded oligonucleotides, from 17 bases in length. It employs a high-salt buffer to bind the negatively charged oligonucleotides to the positively charged spin-tube membrane through centrifugation, so that all other components, including positively charged and neutral ligand molecules would be eluted. PCR-grade water was then used (rather than the manufacturers recommendation of an ethanol-based buffer) to wash any impurities away before elution of the DNA using a low-salt concentration solution. The TRAP assay is sensitive to even trace amounts of ethanol, which was present as residual in the PCR reaction mixture from the spin tube purification step. Even when 1% ethanol was present it was found to severely inhibit the subsequent PCR step. To overcome this problem it was first necessary to freeze-dry the eluted samples in order to remove any traces of ethanol from the purification step. The purified samples were freeze-dried and then redissolved in PCR-grade water at room temperature prior to the second amplification step. *Step 3*: The purified extended samples were then subject to PCR amplification. For this, a second PCR master mix was prepared consisting of ACX reverse primer (1 μM; 5′-GCG CGG [CTTACC]$_3$ CTA ACC-3′), TS forward primer (0.1 μg; 5′-AAT CCG TCG AGC AGA GTT-3′), TRAP buffer, BSA (5 μg), 0.5 mM dNTP and 2U of *TAQ* polymerase (RedHot, ABgene, Surrey, UK). An aliquot of 10 μL of the master mix was added to the purified telomerase extended samples and amplified for 35 cycles of 94 °C for 30 s, at 61 °C for 1 min and 72 °C for 1 min. Samples were separated on a 12% PAGE and visualized with SYBR green (Aldrich) staining. Gels were quantified using a gel scanner and gene tool software (Sygene, Cambridge, UK). Intensity data were obtained by scanning and integrating the total intensity of each PCR product ladder in the denaturing gels. Drug samples were normalized against positive control containing protein only. All samples were corrected for background by subtracting the fluorescence reading of negative controls. Data for all ligands was collected at a range of concentrations in order to obtain dose−response curves, from which EC_{50} values (the concentration required for 50% enzyme inhibition, corresponding to a 50% decrease in total integrated ladder intensity), were obtained by inspection. Graphs were fitted to dose−response curves using the Origin 6.0 software package.

Cellular Proliferation Assay. Short-term growth inhibition was measured using the Sulphorhodamine B (SRB) assay as described previously.[30] Briefly, cells were seeded (4000 cells/wells) into the wells of 96-well plates in DMEM and incubated overnight as before to allow the cells to attach. Subsequently cells were exposed to freshly made solutions of ligand at increasing concentrations and incubated for a further 96 h. Following this the cells were fixed with ice-cold trichloacetic acid (TCA) (10%, w/v) for 30 min and stained with 0.4% SRB dissolved in 1% acetic acid for 15 min. All incubations were carried out at room temperature. The IC_{50} value, the concentration required to inhibit cell growth by 50%, was determined from the mean absorbance at 540 nm for each ligand concentration expressed as a percentage of the control untreated well absorbance.

Synthetic Chemistry. All chemicals were purchased from Sigma-Aldrich and Fisher Scientific and were reagent grade. They were used as supplied without further purification. Solvents were supplied by BDH, Sigma-Aldrich and Fisher Scientific (HPLC grade). Flash chromatography employed Merck silica gel [Kieselgel 60 (0.040−0.063 mm)]. Analytical TLC was performed using 0.2 mm silica-coated aluminum sheets [60 F_{254}] from Merk. ^{1}H NMR and ^{13}C NMR spectra were recorded at 295K on a Bruker Avance 400 spectrometer at 400 and 100 MHz respectively using the specified deuterated solvent purchased from GOSS Scientific or Sigma-Aldrich. NMR spectra were analyzed in MestReC 4.5.6.0 and reported as observed with coupling constants (*J*) in hertz (Hz). Melting points (m.p.) were conducted using a Bibby Stuart Scientific SMP3 melting point apparatus, High resolution accurate mass spectra (HRMS) were conducted on a Micromass Q-TOF Ultima Global tandem mass spectrometer using electrospray ionization mode and 50% acetonitrile in water and 0.1% formic acid as solvent, and processed using the MassLab 3.2 software. All ligands were purified by semipreparative reversed-phase HPLC (Semi-Prep HPLC) on a Gilson chromatograph with a Gilson 215 liquid handler and a Gilson 845Z injection module coupled to a Gilson UV/vis 155 detector and YMC C18 5 μm (100 × 20 mm) column or YMC C18 5 μm (1000 × 30 mm) using 0.1% formic acid in acetonitrile and 0.1% formic acid in water (flow rate: 10 mL min^{-1}). Analytical HPLC analyses were carried out on a Gilson chromatograph with YMC C18 5 μm (100 × 4.6 mm) column and an Agilent 1100 series photodiode array detector (flow rate: 1 mL min^{-1}) to assess

(28) Humphrey, W.; Dalke, A.; Schulten, K. *J. Mol. Graph* **1996**, *14*, 33.
(29) Baker, N. A.; Sept, D.; Joseph, S.; Holst, M.; McCammon, A. J. *Proc. Natl. Acad. Sci. U.S.A.* **2001**, *98*, 10037.
(30) Gowan, S. M.; Harrison, R. J.; Patterson, L.; Valenti, M.; Read, M. A.; Neidle, S.; Kelland, L. R. *Mol. Pharmacol.* **2002**, *61*, 1154.

sample purity. Spectra were processed using the Unipoint 5.11 software package, with compound purity and retention time (t_R) assessed at 254 nm. Compounds were concentrated using freeze drier Savant A160 SpeedVac Concentrator and Vacuubrand CVC 3000. Infrared measurements were carried out on a Perkin-Elmer Spectrum 100 FT-IR spectrometer. Compound names were obtained from CS ChemDraw Ultra 12.0.

3,6-Diazidoacridine (2). 3,6-diaminoacridine hydrochloride (0.50 g, 2.40 mmol) was dissolved in TFA (15 mL) and stirred at 0−5 °C for 10 min. $NaNO_2$ (0.60 g, 8.70 mmol) was then added in small portions and over a period of 5 min, followed by NaN_3 (1.60 g, 25.0 mmol), under vigorous stirring and cooling with ice (special care must be taken during this time to avoid any possible foaming formation). The reaction mixture was stirred for 75 min, followed by the addition of two portions of ice water (2 × 20 mL) to induce the precipitation of the product, which was then collected by filtration (0.06 g, 85%). mp 155−159 °C black dec [Lit.[31] 168−169 °C dec.]. ^{1}H NMR (MeOD, 400 MHz): δ 9.45 (2H, s), 8.31 (2H, d, J = 10 Hz), 7.65 (2H, d, J = 2 Hz), 7.48 (2H, dd, J = 10.2 Hz). IR (film) 2114.36, 1678.21, 1165.72.

4-Chloro-*N*-(3-ethynylphenyl)butanamide (4). To an ice cooled mixture of 3-ethynylbenzenamine (0.72 g, 0.9 mL, 6.14 mmol) and sodium bicarbonate (0.95 g, 11.31 mmol) in DMA (6 mL), 4-chlorobutanoyl chloride (1.59 g, 1.25 mL, 11.30 mmol) was added dropwise and it was vigorously stirred for 75 min. 0.5 M $NaHCO_{3\,aq}$ (8 mL) was slowly added dropwise, keeping the yellow mixture at 0 °C and it was left to stir for 30 min. The white solid was collected by filtration, washed with H_2O and dried overnight, to yield 0.89 g of product (65%). The product was crystallized from hexane/ethyl acetate, 9:1. mp 83−85 °C. ^{1}H NMR ($CDCl_3$, 400 MHz): δ 7.60 (s, 1H), 7.50 (d, J = 7.2 Hz, 1H), 7.23 (m, 3H), 3.67 (m, 2H), 3.03 (s, 1H), 2.53 (m, 2H), 2.17 (m, 2H). ^{13}C NMR ($CDCl_3$, 400 MHz): δ 169.99, 137.67, 129.04, 128.11, 123.24, 122.89, 120.37, 83.04, 77.53, 44.35, 34.10, 27.82. HRMS theoretical $C_{12}H_{12}ClNO$ mass 222.068 $[M+1]^+$, found 222.067.

General Procedure of Synthesis for Compounds 5a−i, 6a−i, and 7a−i. To an ice cooled solution of 3-ethynylbenzenamine in THF and TEA, 2-chloroacetyl chloride (for **5a−i**), 2-chloropropionyl chloride (for **6a−i**), or 4-chloro-*N*-(3-ethynylphenyl)butanamide (for **7a−i**) was added dropwise and the mixture was allowed to warm up to r.t., stirring vigorously for 2 h. The appropriate amine was then added to the ice-cooled mixture and it was stirred overnight, for approximately 17 h at r.t. The THF was removed on a rotary evaporator and the residue was basified (pH = 8.0) with a sat. $NaHCO_{3(aq.)}$ (5 M NH_4OH for **7a−i**) solution and extracted with portions of dichloromethane. The combined fractions were dried over $MgSO_4$ and evaporated *in vacuo*. The crude product was purified by flash column chromatography over silica gel, eluting with dichloromethane, then dichloromethane:methanol (99:1, 97:3, 95:5 for **5a−i**), (99:1, 97:3, 95:5, 93:7 for **6a−i**), or (98:2, 95:5, 90:10 for **7a−i**) The pure compound was further purified by HPLC using the following eluents: A = H_2O and 0.1% FA, B = ACN and 0.1% FA, 0 min (75% A, 25% B), 3 min (75% A, 25% B), 8−15 min (75% A, 25% B). Further details and analytical data are provided as Supporting Information.

General Synthetic Procedures for Compounds 8a−i, 9a−i, and 10a−i. To a suspension of the appropriate building block (**5a−i**, **6a−i**, **7a−i**) and 3,6-diazidoacridine in tBuOH, (+)-sodium L-ascorbate and copper(II) sulfate pentahydrate in H_2O were added in one portion. The heterogeneous mixture was stirred vigorously at room temperature for 3 days and it was then concentrated under reduced pressure. The resulting residue was washed with 1:1 mixture of water/methanol and collected by filtration. The crude product was subjected to preparative HPLC purification, using the following eluents: A = H_2 O and 0.1% FA, B = ACN and 0.1% FA, 0 min (95% A, 5% B), 2 min (95% A, 5% B), 21 min (50% A, 50% B), 23.50 min (95% A, 5% B). Further details and analytical data are provided as Supporting Information; data on the two most active compounds are detailed below.

***N*,*N*′-((1,1′-(Acridine-3,6-diyl)bis(1*H*-1,2,3-triazole-4,1-diyl))bis(3,1-phenylene))bis(3-(pyrrolidin-1-yl)propanamide) (9a).** To a suspension of *N*-(3-ethynylphenyl)-3-(pyrrolidin-1-yl)propanamide (0.14 g, 0.58 mmol) and 3,6-diazidoacridine (0.07 g, 0.27 mmol) in 2 mL of tBuOH, a solution of (+)-sodium L-ascorbate (0.026 g, 0.135 mmol) and copper(II) sulfate pentahydrate (0.007 g, 0.027 mmol) in 2 mL of H_2O was added in one portion. The heterogeneous mixture was treated according to the general procedure to afford a dark brown solid (0.142 g, 82%). Purity by HPLC analysis, 99% (t_R = 18.13 min). mp >275 °C. ^{1}H NMR (TFA+D_2O, 400 MHz): δ 13.43 (1H, s), 12.65−12.56 (4H, m), 12.23 (2NH, s), 12.01−12.00 (2H, m), 11.63−11.58 (4H, m), 11.16−11.15 (2H, m), 11.02−10.86 (4H, m), 7.29−7.28 (2H, br s), 7.01−7.00 (2H, br s), 6.48−6.44 (10H, m), 5.61 (6H, br s), 5.20−5.18 (4H, m). HRMS theoretical $C_{43}H_{43}N_{11}O_2$, mass 746.367 $[M+1]^+$, found 746.370.

***N*,*N*′-((1,1′-(Acridine-3,6-diyl)bis(1*H*-1,2,3-triazole-4,1-diyl))bis(3,1-phenylene))bis(3-(diethylamino)propanamide) (9b).** To a suspension of 3-(diethylamino)-*N*-(3-ethynylphenyl)propanamide (0.142 g, 0.58 mmol) and 3,6-diazidoacridine (0.07 g, 0.27 mmol) in 2 mL of tBuOH, a solution of (+)-sodium L-ascorbate (0.026 g, 0.135 mmol) and copper(II) sulfate pentahydrate (0.007 g, 0.027 mmol) in 2 mL of H_2O was added in one portion. The heterogeneous mixture was treated according to the general procedure to afford a dark brown solid (0.16 g, 78%). Purity by HPLC analysis, 98% (t_R = 16.88 min). mp >275 °C. ^{1}H NMR (TFA+D_2O, 400 MHz): δ 12.34 (1H, s), 11.64 (2H, s), 11.12−11.10 (2H, m), 10.91 (2H, br s), 10.47 (2H, s), 10.37 (2H, s), 10.26 (2NH, s), 10.04 (2H, br s), 9.88 (2H, br s), 9.77 (2H, br s), 5.82 (4H, s), 5.63 (8H, br s), 5.37 (4H, s), 3.68−3.66 (12H, m). ^{13}C NMR (TFA+D_2O, 400 MHz): δ 167.11, 162.54, 146.84, 138.05, 136.45, 132.41, 129.67, 126.61, 122.94, 120.73, 120.54, 119.71, 118.51, 117.38, 115.71, 44.32, 43.53, 24.28, 2.08. HRMS theoretical $C_{43}H_{47}N_{11}O_2$, mass 750.399 $[M+1]^+$, found 750.398.

Acknowledgment. S.S. is a Maplethorpe Fellow of The University of London. This work was supported by Programme Grant No. C129/A4489 to S.N. from Cancer Research UK, and by the FP6 framework grant "Molecular Cancer Medicine" from the EU.

Supporting Information Available: Analytical and synthetic data on intermediate compounds **5a−i**, **6a−i**, **7a−i**, **8a−i**, **9a−i**, and **10a−i**. This material is available free of charge via the Internet at http://pubs.acs.org.

JA1003944

(31) Firth, W. *J. Org. Chem.* **1982**, *47*, 3002.